Effect of KOH concentration and growth of platinum nanoparticles on current collector to improved performance of supercapacitor cells

R. Farma[*], R. R. Hasibuan, A. Awitdrus, Y. Hamzah, E. Taer, A. Apriwandi
Department of Physics, Faculty of Mathematics and Natural Sciences, University of Riau, 28293 Simpang Baru, Riau, Indonesia

This research aims to determine the effect of KOH concentration on the electrochemical properties of activated carbon from raw fibers of oil palm empty fruit bunches (OPEFB) and the effect of platinum nanoparticles growth of stainless steel on a current collector electrode supercapacitor. Furthermore, varying KOH concentrations of 0.3, 0.6, and 0.9 M were used to conduct that the chemical and physical activation processes using N_2 and CO_2 gas at 600°C and 700°C, respectively. Furthermore, platinum nanoparticles were grown on the surface stainless steel current electrode by using a simple wet chemical method to improve the performance of supercapacitors Therefore, to achieve, KOH concentration on the morphology, adsorption, and electrochemical properties of the obtained electrode were investigated. Furthermore, many spherical platinum shapes ranging from 20 to 100 nm were observed through FESEM, while the high specific surface area of the carbon electrodes was confirmed by using the N_2 adsorption-desorption isotherm at 77K. In addition, the surface areas of both carbon electrodes were measured at 395 and 373 m^2 g^{-1} for KOH concentration using 0.9 M and 0.6 M, respectively. The results showed that the cyclic voltammetry (CV) of the modified supercapacitor electrode with platinum nanoparticles increased the specific capacitance with the highest value at 149.63 F g^{-1}.

1. Introduction

The utilization of batteries as an energy storage device is considered less efficient, due to its several weaknesses, such as small power density and long electrical storage time [1]. This led to the discovery of the supercapacitor, which has the ability to save higher energy and power density over a prolonged life cycle. This device consists of four main components, namely electrolyte, separator, current collector, and electrode [2,3]. The electrode is the most important component used to determine its performance, which is made from a metal oxide, polymer, and carbon [4,5]. Over the years, activated carbon has been widely used as a supercapacitor electrode due to its numerous advantages such as high surface area, cost-effectiveness, and its availability in large quantities [6]. The fabrication of supercapacitor cells using activated carbon as the electrode is generally derived from biomass such as mangosteen [7], coffee [8], pineapple crown [9], basil seed [10]. However, in this study, the electrodes were made from fibers of oil palm empty fruit bunches with a combination of KOH and CO_2 activation. In addition, the current collector is also an important component with platinum nanoparticles grown on the surface to improve its performance. This research, therefore, aims to observe the effect of molarity concentration of KOH and platinum nanoparticles on the performance of supercapacitor.

---

[*] Corresponding author: rakhmawati.farma@lecturer.unri.ac.id

2. Experimental

2.1. Synthesis of activated carbon and growth nanoparticle

The activated carbons were prepared from OPEFB through the combination of chemical and physical activation. Furthermore, potassium hydroxide (KOH) was used as an activation agent with three varying concentrations, of 0.3, 0.6, and 0.9 M. The carbonization process was conducted using N_2 at 600°C, and activated with CO_2 at 700°C with 1 l/min flow rate. The platinum nanoparticles were grown on the surface of stainless steel at 316 L, with the solution prepared by mixing 1 mL of 0.01 M of K_2PtCl_4 in 18 mL of DI water mixed with 1 mL of a 0.2 ascorbic acid solution ($C_6H_8O_6$). In addition, the stainless steel was soaked in the platinum nanoparticle solution for 4 hours, rinsed with DI water, and dried with N_2 gas.

2.2. Characterizations

The morphological properties of the stainless steel current collector were conducted by scanning the field effect of the electron microscope (FESEM) (Zeiss SUPRA 55VP). Furthermore, the porosity parameter of the electrodes, such as the BET surface area and isotherm of adsorption-desorption of N_2 at 77K, were measured using Quantachrome NovaWin (Quantachrome Instrument version 11.0). While the electrochemical property of the supercapacitor cell was investigated using the cyclic voltammetry method using Physics CV UR Rad-Er 5841. The specific capacitance of supercapacitor was determined using the following equation:

$$C_{sp} = \frac{2[(I_c - I_d)/2]}{s\,m} \tag{1}$$

where I_c is a current charge, I_d is current discharge, s is scan rate, and m is mass of carbon electrode.

3. Results and discussions

3.1. Physical properties analysis

Fig. 1(a, b, c) shows the comparison of the FESEM micrograph of the surface morphological of the electrodes with varying KOH molarity concentration of 0.3, 0.6 and 0.9 M, respectively, at a magnificent rate of 20000 times. These micrographs clearly showed that all carbon electrodes are porous with numerous meso/macropores with different sizes and shapes between the grains and boundaries. Interestingly, Fig. 1(c) performed hierarchical meso/macroporous compared to Fig. 1(a) and (b) which contributed to facilitate the rich-active site and more rate diffusion ions to electrode/electrolyte interface [11]. Therefore, the carbon electrode with a concentration of 0.9 M has a higher specific surface area and capacitance. Similarly, the smaller macropores on the surface and inside the grains are not visible in the micrograph at this magnification. Furthermore, the porosity of carbon electrodes increases with rise in the molarity concentration of KOH [12,13].
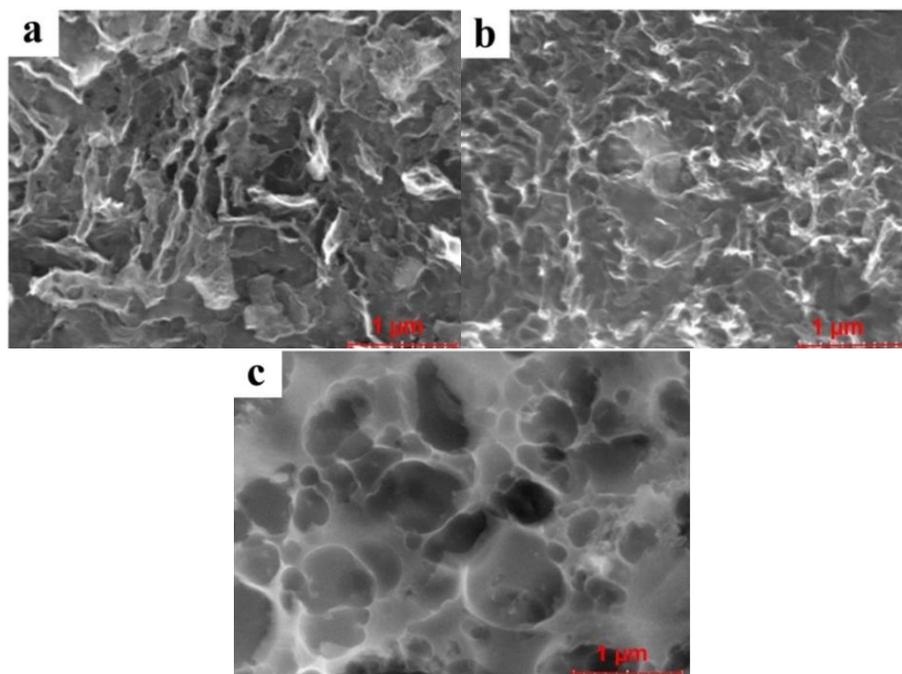
Fig. 1. Surface morphology of carbon electrode at a magnificent rate of 20000 times for samples of (a) 0.3 M, (b) 0.6 M and (c) 0.9 M.

According to Inagaki *et al.,* [14] an increase in specific capacitance by chemical activation using KOH is caused by changes to the surface shape of the carbon electrode, which was affected by the amount of ions in the electrolyte solution capable of penetrating into its micro and mesopores. These elements tend to allow the ions of electrolyte solution into the pores of the electrode to create a double layer [15,16].
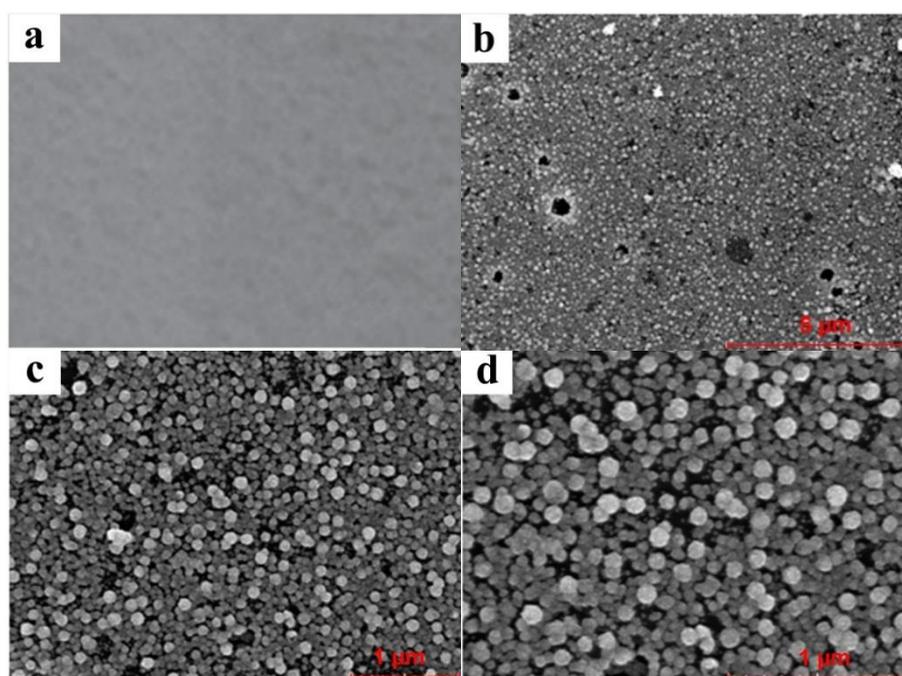
Fig. 2. (a) Stainless steel current collector, (b) Platinum nanoparticles on the surface of stainless steel with magnification of 10,000 times, (c) 30,000 times, and (d) 50,000 times.

The surface morphology of stainless steel current collector before and after the growth of platinum nanoparticles at the magnificence of 10,000 times, 30,000, and 50,000 times, respectively, as shown in Fig. 2. The platinum nanoparticles were evenly distributed throughout the surface of the stainless steel current collector, as shown in Fig. 2(b), and (c). Its presence showed that the growth occurred successfully, and the platinum nanoparticles were uniformly distributed throughout the surface of the stainless steel current collector. The shape of platinum nanoparticles is spherical, with the particle sizes ranging approximately from 20 to 100 nm. Furthermore, its spherical shape is consistent with the research conducted by Cao *et al.,* [17], which stated that platinum nanoparticles grow on the surface of the carbon electrode.

Furthermore, The N_2 adsorption and desorption isotherm at 77 K data for the carbon electrodes with a variation of KOH concentration is shown in Fig. 3. According to IUPAC standardization, all isotherm data are type IV profile [4,18]. The IV type marked a hysteresis loop in the range of 0.40-0.9 P/P0 relative pressure, which showed that the material is mesoporous [19]. The isotherm curve character with a sudden increase in the adsorbed volume and a rounded knee is in the lower relative pressure range. Therefore, all the electrodes possess a wide pore size distribution, which ranged from micropore to mesopore. The specific surface areas of electrode carbon are 395 m^2 g^{-1} and 373 m^2 g^{-1} at 0.9 M and 0.6 M KOH, respectively.
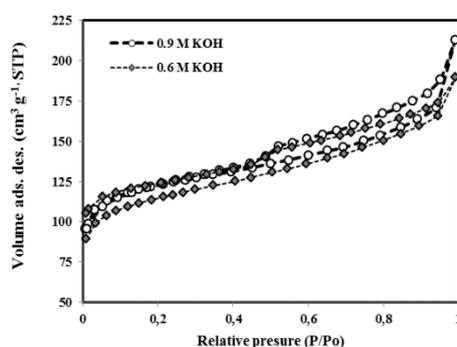
Fig. 3. N_2 adsorption-desorption isotherm of carbon electrode treated with 0.6 M and 0.9 M KOH.

3.2. Electrochemical properties analysis

The specific capacitances of the supercapacitors were measured using the cyclic voltammetry method at voltage window of 0-0.5 V in 1 M H_2SO_4 aqueous electrolyte. Fig. 4 shows the cyclic voltammogram of supercapacitor cells with the electrode from KOH concentration of 0.3 M, 0.6 M, and 0.9 M, without the growth of platinum nanoparticle. The CV curves of all samples presented quasi-rectangular shapes that confirmed good electrochemical double-layer behaviour with no obvious pseudo-capacitive effect [20,21]. Furthermore, a larger curve area of higher specific capacitance was formed [22,23]. By using standard formula, the specific capacitances of porous carbon with KOH impregnation of 0.3 M, 0.6 M, and 0.9 M, without growth of platinum nanoparticle are 128.58 F g^{-1}, 132.77 F g^{-1}, and 140.79 F g^{-1}, respectively. This is speculated higher molarities of KOH were enhanced the capacitive properties of symmetric supercapacitor from 128.58 F g^{-1} to 140.79 F g^{-1}. Moreover, the growth of platinum nanoparticles on the surface of the stainless steel current collector affected the specific capacitance of the supercapacitor cell, which increased, as shown in Fig. 5. In addition, the CV profiles in Fig.5 retain the quasi-rectangular type which confirmed the normal electrochemical double-layer properties. The platinum nanoparticles also affected its performance, which increased after the growth on the surface of stainless steel due to the contact between the current collector containing platinum nanoparticles and the surface of the carbon electrode, which decreased the equivalent resistant series.
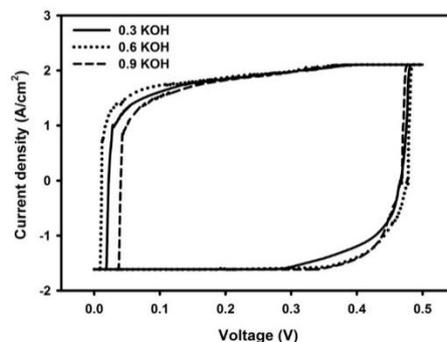
Fig. 4. Cyclic voltammogram of the supercapacitor cell without platinum nanoparticle.

The movement of I_c to the positive direction in the voltammogram curve was also accompanied by the movement of I_d to the negative direction. The changes in I_c and I_d were due to the enhancement of the capacitive properties of supercapacitor cells [24,25]. The specific capacitance of the supercapacitor cells is shown in Table 1.
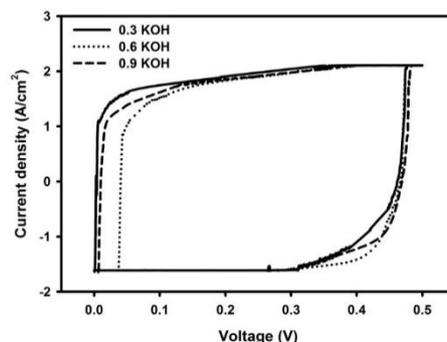
Fig. 5. Cyclic voltammogram of supercapacitor cells after growth of platinum nanoparticle on the surface of stainless steel current collector.

Table 1. The specific capacitance of supercapacitor cells after growth of platinum nanoparticle on the surface of stainless steel current collector with the scan rate of 1 mV s^{-1}.

Samples	Mass (g)	C_{sp} (F/g)
0.3 M	0.02412	149.63
0.6 M	0.02561	137.05
0.9 M	0.02493	141.24

4. Conclusions

In conclusion, the platinum metal-based material deposited on the current collector by the wet-chemical method was successfully grown on the surface of stainless steel. Its morphology showed the ability to be distributed with a spherical shape in size range of 20–100 nm. The CV charge-discharge of the modified electrode after the growth of platinum nanoparticles increased the super-capacitive performance compared to the current collector without platinum. Based on the modified electrode, the molality concentration of the KOH ratio 0.3 M showed a good maximum specific capacitance of 149.63 F g^{-1} at a scan rate of 1 mV s^{-1}.

Acknowledgments

The authors are grateful to the DRPM Kemenristek/BRIN, Republic of Indonesia for financial support through first year project of DPUPT.

References

[1] H. Yang, S. Ye, J. Zhou, T. Liang, Front. Chem. **7**, 1 (2019).

[2] Poonam, K. Sharma, A. Arora, S. K. Tripathi, J. Energy Storage **21**, 801 (2019).

[3] E. Taer, R. Taslim, in AIP Conf. Proc., 020004-1 (2018).

[4] R. T. Ayinla, J. O. Dennis, H. M. Zaid, Y. K. Sanusi, F. Usman, L. L. Adebayo, J. Clean. Prod. **229**, 1427 (2019).

[5] K. Dhara, D. R. Mahapatra, J. Mater. Sci. **54**, 12319 (2019).

[6] Z. Gao, Y. Zhang, N. Song, X. Li, Mater. Res. Lett. **5**, 69 (2017).

[7] V. Yang, R.A. Senthil, J. Pan, A. Khan, S. Osman, L. Wang, W. Jiang, Y. Sun, J. Electroanal. Chem., 113616 (2019).

[8] Y. H. Chiu, L. Y. Lin, J. Taiwan Inst. Chem. Eng. **101**, 177 (2019).

[9] E. Taer, A. Apriwandi, Y. S. Ningsih, R. Taslim, Agustino, Int. J. Electrochem. Sci. **14**, 2462 (2019).

[10] H. Yang, J. Zhou, M. Wang, S. Wu, W. Yang, H. Wang, Int. J. Energy Res. **44**, 4449 (2020).

[11] A. R. Selvaraj, A. Muthusamy, Inho-Cho, H.J. Kim, K. Senthil, K. Prabakar, Carbon N. Y. **174**, 463 (2021).

[12] S. Kumagai, M. Sato, D. Tashima, Electrochim. Acta **114**, 617 (2013).

[13] Q. Sun, T. Jiang, G. Zhao, J. Shi, Int. J. Electrochem. Sci. **14**, 1 (2019).

[14] M. Inagaki, H. Konno, O. Tanaike, J. Power Sources **195**, 7880 (2010).

[15] Y. Liang, Y. Lu, G. Xiao, J. Zhang, H. Chi, Y. Dong, Appl. Surf. Sci. **529**, 147141 (2020).

[16] S. Yousaf, M. Aadil, S. Zulfiqar, M.F. Warsi, P.O. Agboola, M.F. Aly Aboud, I. Shakir, J. Mater. Res. Technol. **9**, 14158 (2020).

[17] W. Cao, F. Yang, Mater. Today Energy **9**, 406 (2018).

[18] E. E. Miller, Y. Hua, F. H. Tezel, J. Energy Storage **20**, 30 (2018).

[19] J. Jose, V. Thomas, V. Vinod, R. Abraham, S. Abraham, J. Sci. Adv. Mater. Devices **4**, 333 (2019).

[20] C. Ma, Q. Fan, M. Dirican, N. Subjalearndee, H. Cheng, J. Li, Y. Song, J. Shi, X. Zhang, Appl. Surf. Sci. **545**, 148933 (2021).

[21] T. Yumak, G.A. Yakaboylu, O. Oginni, K. Singh, E. Ciftyurek, E. M. Sabolsky, Colloids Surfaces A Physicochem. Eng. Asp. **586**, 124150 (2020).

[22] R. Farma, M. Deraman, A. Awitdrus, I.A. Talib, E. Taer, N. H. Basri, J. G. Manjunatha, M. M. Ishak, B. N. M. Dollah, S. A. Hashmi, Bioresour. Technol. **132**, 254 (2013).

[23] G. Gou, F. Huang, M. Jiang, J. Li, Z. Zhou, Renew. Energy **149**, 208 (2020).

[24] E. Taer, A. Apriwandi, R. Taslim, U. Malik, Z. Usman, Int. J. Electrochem. Sci. **14**, 1318 (2019).

[25] S. Faraji, F. Nasir, Renew. Sustain. Energy Rev. **42**, 823 (2015).